Journal of Orthopaedic Translation 49 (2024) 82–95

Contents lists available at ScienceDirect

Journal of Orthopaedic Translation

journal homepage: www.journals.elsevier.com/journal-of-orthopaedic-translation

Original Article

The CD163/TWEAK/Fn14 axis: A potential therapeutic target for alleviating inflammatory bone loss

Ji-kun Qian [a,b,1], Yuan Ma [b,1], Xuan Huang [c,1], Xiao-ran Li [c], Ya-fei Xu [a], Zi-ying Liu [c], Yuan Gu [b], Ke Shen [b], Liang-jie Tian [b], Yu-tian Wang [b], Ning-ning Cheng [d], Bing-sheng Yang [b], Kui-yuan Huang [e], Yu Chai [b], Guan-qiao Liu [b], Nai-qian Cui [b], Song-yun Deng [f], Nan Jiang [b,***], Dao-rong Xu [b,**], Bin Yu [b,*]

[a] Division of Orthopaedics and Traumatology, Department of Orthopaedics, The Seventh Affiliated Hospital, Southern Medical University, Foshan, 528200, China
[b] Division of Orthopaedics and Traumatology, Department of Orthopaedics, Nanfang Hospital, Southern Medical University, Guangzhou, 510515, China
[c] Guangdong Provincial Key Laboratory of Viral Hepatitis Research, Department of Infectious Diseases, Nanfang Hospital, Southern Medical University, Guangzhou, 510515, China
[d] Department of Obstetrics, The First Affiliated Hospital, Guangzhou University of Chinese Medicine, Guangzhou, 510405, China
[e] Department of Gastroenterology, The Second Affiliated Hospital of Nanchang University, Nanchang, Jiangxi, 330000, China
[f] Department of Orthopaedics and Traumatology, Zhujiang Hospital, Southern Medical University, Guangzhou, 510280, China

ARTICLE INFO

Keywords:
Bone homeostasis
CD163
Inflammation
Osteoporosis
Osteoclast
TWEAK

ABSTRACT

Objective: Osteoclast (OC) over-activation is an important cause of bone loss that is strongly correlated with inflammation. Although the CD163/TWEAK/Fn14 axis has been implicated in several inflammatory pathologies, its contributions to inflammatory bone loss remain poorly understood. This study aimed to evaluate the interaction of the CD163/TWEAK/Fn14 axis with OC in inflammatory bone loss.

Methods: To assess the role of CD163 in bone homeostasis, we characterized the bone phenotypes of CD163-deficient mice and their wild-type littermates. CD163 and TWEAK levels were evaluated in the bone marrow of mice with LPS-induced bone loss and individuals with rheumatoid arthritis (RA). Bone mass changes were assessed using uCT and histology following supplementation with recombinant mouse CD163 protein (rCD163) or blockade of TWEAK/Fn14 signaling in CD163-deficient mice and mice with LPS-induced bone loss. The impact of CD163/TWEAK on OC differentiation and bone resorption capacity was analyzed *in vitro*.

Results: CD163 deficiency caused decreased bone mass and increased OC abundance. Lower CD163 expression and higher TWEAK expression were observed in the bone marrow of mice with LPS-induced bone loss and individuals with RA. TWEAK, mainly derived from $CD68^{+}$ macrophages, was responsible for bone loss, and supplementing rCD163 or blocking TWEAK/Fn14 signaling contributed to rescue bone loss. TWEAK/Fn14 synergistically promoted RANKL-dependent OC differentiation and bone resorption capability through downstream mitogen-activated protein kinases (MAPK) signaling, while the pro-osteoclastic effect of TWEAK was suppressed by CD163.

Conclusion: Our findings suggest that the CD163/TWEAK/Fn14 axis is a potential therapeutic target for inflammatory bone loss by regulating osteoclastogenesis.

* Corresponding author. Division of Orthopaedics and Traumatology, Department of Orthopaedics, Nanfang Hospital, Southern Medical University, No.1838 North of Guangzhou Avenue, Baiyun District, Guangzhou, Guangdong Province, 510515, China.
** Corresponding author. Division of Orthopaedics and Traumatology, Department of Orthopaedics, Nanfang Hospital, Southern Medical University, No.1838 North of Guangzhou Avenue, Baiyun District, Guangzhou, Guangdong Province, 510515, China.
*** Corresponding author. Division of Orthopaedics and Traumatology, Department of Orthopaedics, Nanfang Hospital, Southern Medical University, No.1838 North of Guangzhou Avenue, Baiyun District, Guangzhou, Guangdong Province, 510515, China.
E-mail addresses: hnxyjn@smu.edu.cn (N. Jiang), xhuang2000@smu.edu.cn (D.-r. Xu), yubin@smu.edu.cn (B. Yu).
[1] These authors contributed equally to this work.

https://doi.org/10.1016/j.jot.2024.09.002
Received 17 March 2024; Received in revised form 21 August 2024; Accepted 1 September 2024

The translational potential of this article

Supplementation with rCD163 or up-regulation of CD163 expression to enhance the body's anti-osteoporotic and anti-inflammatory capacity may be an alternative strategy for managing inflammatory bone loss.

1. Introduction

Inflammation is a key factor in systemic or localized bone loss during aging and in chronic diseases, including rheumatic diseases, periodontitis, arthritis, periprosthetic loosening, and infectious osteomyelitis [1–3]. In addition to structural and functional damage to joints, patients with rheumatoid arthritis (RA) also experience severe periarticular bone loss and systemic osteoporosis [4]. Although current medical treatments can ameliorate inflammation, measures for the management of chronic inflammatory responses are limited, resulting in a silent and progressive loss of bone mass that ultimately leads to disability and mortality [5–7]. Therefore, elucidating the events and factors involved in inflammatory bone loss are crucial to enhancing the current understanding of these diseases and fostering the development of novel preventive and therapeutic strategies.

Over-activation of osteoclasts (OCs) is considered to be one of the main mechanisms involved in inflammatory bone loss [8,9]. RANKL binding to RANK triggers the activation of TNF receptor-associated factor 6-mediated mitogen-activated protein kinases (MAPK) and nuclear factor-kappa-B (NF-κB) signaling pathways to regulate nuclear factor of activated T cells c1 (NFATc1) and OC-associated functional proteins, ultimately initiating OC formation [10,11]. During inflammation, several immune cells, including macrophages, become activated and secrete a wide range of osteolytic cytokines that enhance RANKL-dependent or -independent osteoclastogenesis, which worsens bone loss [6,12,13]. Macrophages also directly participate in OC differentiation as OC precursors (OCPs) [10]. Although blocking RANKL signaling—either directly with anti-RANKL neutralizing antibodies or indirectly through cytokine suppression—reduces bone loss, many osteoporosis sufferers remain resistant to current treatments [14–16]. Thus, effective treatments that target OCs in the inflammatory environment to alleviate osteolysis are limited.

CD163 is a member of the type I transmembrane scavenger receptor family and is expressed exclusively on monocytes and macrophages; hence, it is widely regarded as a marker for alternatively activated M2-type macrophages [17,18]. Recent studies reported that $CD163^{+}$ macrophages form a unique subpopulation of bone marrow-resident macrophages (BMRMs) with both immunomodulatory and antimicrobial properties [19]. CD163 also serves as a decoy receptor for tumor necrosis factor-like weak inducer of apoptosis (TWEAK) [20,21]. TWEAK is a multifunctional pro-inflammatory cytokine that is mainly expressed by macrophages/monocytes under inflammatory conditions and regulates a series of cellular activities upon binding to the downstream receptor fibroblast growth factor-inducible 14 (Fn14) [22–24]. In addition, CD163 and TWEAK exist in both membrane bound and soluble forms (sCD163, sTWEAK) due to protease-mediated shedding of the extracellular structural domains [25].

There is increasing evidence that TWEAK/Fn14 signaling plays a pivotal role in inflammatory diseases. Uncontrolled chronic inflammation leads to prolonged and excessive activation of the TWEAK/Fn14 signaling pathway, which further exacerbates the pathological response in disorders [24,26–28]. In cardiovascular diseases, $CD163^{+}$ macrophages internalize and degrade TWEAK to impair the progression of atherosclerotic plaques [25,28]. In mice with collagen-induced arthritis, CD163 deficiency worsens joint inflammation and bone destruction [29,30]. TWEAK has been reported to promote RANKL expression in synovial fibroblasts and sclerostin expression in human osteoblasts, which promote bone resorption and inhibit bone formation, respectively [31,32]. However, the role of CD163 in inflammatory bone loss has not been adequately investigated, and the exact impact of the CD163/TWEAK/Fn14 interactions on osteoclastogenesis remains unclear.

In this study, we investigated the impact of CD163 deficiency on TWEAK levels and inflammatory bone loss. The absence of $CD163^{+}$ BMRMs increases TWEAK availability, favoring its interaction with Fn14. The up-regulation of TWEAK/Fn14 signaling in OCPs contributes to inflammatory bone loss. Supplementation with recombinant mouse CD163 protein (rCD163) or blockade of TWEAK/Fn14 signaling alleviates lipopolysaccharide (LPS)-induced inflammatory bone loss, which may serve as a potential therapeutic strategy for preventing inflammatory bone loss.

2. Materials and methods

2.1. Mice

CD163 global knockout ($CD163^{-/-}$) and their Wild-type littermates (WT, $CD163^{+/+}$) mice with the C57BL/6 background were purchased from Shanghai Model Organisms Center, Inc (Shanghai, China). C57BL/6 mice were purchased from Southern Medical University Animal Center (Guangzhou, China). All the mice were kept in a specific, pathogen-free animal facility with a sterilized diet and autoclaved water. All animal experiments and procedures were approved by the Animal Care and Use Committee of Nanfang Hospital, Southern Medical University (NFYY-2022-0237).

2.2. Human samples

This study was approved by the Ethics Committee for Human Studies of Nanfang Hospital, Southern Medical University (NFEC-2020-074). All participants involved in this study provided signed informed consent. This study was performed in accordance with the principles of the Declaration of Helsinki. The bone marrow samples were obtained from sites adjacent to inflamed joints in individuals who fulfilled the 2010 ACR/EULAR Rheumatoid Arthritis classification criteria and underwent knee arthroplasty or ankle arthrodesis. The control group comprised individuals who fulfilled the following criteria: had closed fractures of the femur or tibia requiring intramedullary nail fixation by reaming technique; female participants were aged 18–40 years; and male participants were aged 18–50 years with no underlying diseases. Only bone marrow samples from the participants were used for Western blotting analysis in this study.

2.3. Experimental mouse model and treatments

To assess whether TWEAK is responsible for the osteoporotic phenotype of $CD163^{-/-}$ mice, 4-week-old male $CD163^{-/-}$ mice were divided into two groups randomly (n = 8). One group was treated with Ultra-LEAF Purified Rat IgG isotype (1 μg/g/day, RTK2071, BioLegend, California, USA) administered intraperitoneally, while the other group received TWEAK blocking antibody (1 μg/g/day, MTW-1, 120010, BioLegend, California, USA) daily for 28 days. The dosage was determined according to a combination of the manufacturer's recommendations and a previous report [33]. After 28 days, the mice were sacrificed to obtain femora for micro-computed tomography (μCT) analysis.

To explore whether the TWEAK infusion could reproduce the osteoporotic phenotype observed in $CD163^{-/-}$ mice and if CD163 could rescue TWEAK-induced bone loss, recombinant mouse TWEAK protein (rTWEAK) and/or rCD163 were administered intraperitoneally to 8-week-old WT male mice for 28 days. rTWEAK and rCD163 mimic the structures of sTWEAK and sCD163, respectively [33]. After 28 days, the mice were sacrificed to obtain femora for μCT analysis. Mice were randomly separated into three groups (n = 10): vehicle group treated with 0.1 % BSA, rTWEAK group treated with rTWEAK (25 ng/g/day, 50174-M15H, Sino Biological, Beijing, China), and rTWEAK plus rCD163 group treated with both rTWEAK and rCD163 (25 ng/g/day,

RP02115, Abclonal, Wuhan, China).

To determine whether supplementation with rCD163 could reverse bone loss caused by CD163 deficiency, rCD163 was administered intraperitoneally to naive 4-week-old male $CD163^{-/-}$ mice. After 28 days, the mice were sacrificed to obtain femora for μCT analysis. $CD163^{-/-}$ mice were randomly divided into two groups (n = 10): the vehicle group treated with 0.1 % BSA and the rCD163 group treated with rCD163 (25 ng/g/day).

To investigate the contribution of the CD163/TWEAK/Fn14 axis in models of inflammatory bone loss, an established model of LPS-induced chronic inflammatory bone loss was applied with minor modifications [34]. 8-week-old male mice were randomly divided into five groups (n = 10): the vehicle group treated with 0.1 % BSA; the LPS group treated with LPS (3 μg/g, L2630, Sigma–Aldrich, Missouri, USA); the LPS plus rCD163 group treated with both LPS and rCD163 (25 ng/g/day); the LPS plus Aurintricarboxylic acid (ATA) group treated with both LPS and ATA (10 μg/g, HY-122575, MedChemExpress, New Jersey, USA); and the LPS plus low-dose dexamethasone (Dex-L) group treated with both LPS and Dex-L (0.02 ug/g, HY-14648A, MedChemExpress, New Jersey, USA). LPS and Dex-L were administered every 3 days for 4 weeks; rCD163 was administered daily for 4 weeks; and ATA intervention began in the second week after LPS modeling and was administered every 3 days for 3 weeks. After 4 weeks, femora were collected for μCT analysis.

We also analyzed the in situ expression of CD163 in bone marrow tissues of ovariectomized (OVX) mice. Briefly, female mice aged 10 weeks underwent either bilateral oophorectomy (n = 10) or sham surgery (n = 10). The mice were euthanized 8 weeks after surgery, and their femora were collected for further histological analysis.

2.4. μCT analysis

Femora isolated from mice were fixed in 4 % paraformaldehyde for 24 h and scanned using Bruker Micro-CT Skyscan 1276 system (Kontich, Belgium). The scan settings were as follows: voxel size 6.5 μm, medium resolution, 70 kV, 200 μA, Al 0.25 mm filter, and integration time of 350 ms. Images were analyzed and reconstructed using the manufacturer's evaluation software (NRecon, CTan, Bruker, Belgium). For trabecular bone analysis, the region of interest was demarcated as a 2-mm-thick section of the distal femur, located 0.5 mm below the growth plate. As for cortical bone, the region of interest was identified as a 1-mm-thick segment of the mid-femur.

2.5. Histological analysis

Mice were anesthetized and perfused intracardially with 4 % paraformaldehyde. Isolated femora were fixed with 4 % paraformaldehyde overnight at 4 °C, followed by decalcification in pH 7.4, 0.5 M EDTA for 10 days, and paraffin embedding. The femoral paraffin blocks were cut into 4-μm sections and stained with tartrate-resistant acid phosphatase (TRAP/ALP Stain Kit, 294–67001, Fujifilm WAKO, Japan) according to the manufacturer's instructions. The $TRAP^{+}$ multinucleated cells containing at least three nuclei were defined as OCs using Olympus BX63 microscopy (Olympus, Tokyo, Japan). The number of OCs per trabecular bone surface (N. $TRAP^{+}$/mm) was quantified using Olympus cellSens Standard imaging software.

2.6. Immunohistochemistry and immunofluorescence staining

For immunohistochemistry, after deparaffinization and rehydration, antigen retrieval was performed by incubating the sections in EDTA antigen retrieval solution (pH 9.0, ZLI-9069, ZSGB-Bio, Beijing, China) at 65 °C for 3 h, followed by quenching endogenous peroxidase activity in 3 % H_2O_2 for 15 min. After blocking with 10 % goat serum for 1 h at room temperature, the sections were incubated overnight at 4 °C with the following antibodies: anti-NFATc1 (A1539, Abclonal, Wuhan, China), anti- Cathepsin K (CtsK, A1782, Abclonal, Wuhan, China), anti-osteocalcin (Ocn, DF12303, Affinity, Hangzhou, China), anti-CD163 (16646-1-AP, Proteintech, Wuhan, China), or anti-TWEAK (DF7444, Affinity, Hangzhou, China). Afterwards, the sections were incubated with horseradish peroxidase (HRP) anti-rabbit IgG antibody (PV-6001, ZSGB-Bio, Beijing, China) for 1 h at room temperature. Finally, the peroxidase activity of sections was revealed with a DAB substrate kit (ZLI-9017, ZSGB-Bio, Beijing, China) and sections were lightly counterstained with hematoxylin.

For immunofluorescence staining, the decalcified samples were sequentially dehydrated in a 20 % sucrose solution containing 2 % polyvinylpyrrolidone (P5288, Sigma–Aldrich, Missouri, USA) and a 30 % sucrose solution containing 2 % polyvinylpyrrolidone for 24 h. The samples were then embedded in OCT and 10 μm-thick coronal sections were used for immunofluorescence staining. Sections were permeablized for 10 min using 0.3 % Triton-100, then washed in PBS and blocked with 10 % goat serum for 1 h. Slides were stained overnight with combinations of the following antibodies: anti-CD68 (ABM40050, Abbkine, Wuhan, China), anti-F4/80 (71299, CST, Massachusetts, USA), anti-TWEAK (DF7444), or anti-Vpp3 (sc-55544, Santa Cruz, California, USA), anti-Fn14 (ET1611-93, HuaBio, Hangzhou, China). Slides were washed three times in PBS and then incubated with fluorescence-conjugated secondary antibodies at room temperature for 1 h. Fluorescence-conjugated secondary antibodies included Alexa Fluor 594-conjugated goat anti-rabbit IgG (8889, CST, Massachusetts, USA), Alexa Fluor 488-conjugated goat anti-rat IgG (4416, CST, Massachusetts, USA), or iFluor™ 488 conjugated goat anti-mouse IgG (HA1125, HuaBio, Hangzhou, China). Sections were counterstained using DAPI (S2110, Solarbio, Beijing, China) to stain the nuclei before they were mounted and sealed with nail polish. All the sections were observed under an Olympus BX63 microscope (Olympus, Tokyo, Japan).

2.7. ELISA

After anesthetizing the mice with isoflurane, blood samples were obtained through retro-orbital sinus bleeding using a capillary tube. To obtain serum, blood samples were allowed to clot for 3 h at room temperature, followed by centrifugation for 15 min at 1000 g. Serum samples were dispensed and stored at −80 °C until use. The concentration of sTWEAK in serum samples were measured using a commercial mouse TWEAK ELISA kit (EL023987MO, CUSABIO, Wuhan, China) according to the manufacturer's directions.

2.8. Flow cytometry

Surface and intracellular staining of murine immune cells were performed as described previously [35]. After preparing single-cell suspensions of mouse bone marrow cells, the samples were stained with combinations of the following antibodies: anti-CD68-AF488 (53-0681-82), anti-CD19-FITC (11-0193-81), anti-F4/80-FITC (11-4801-81), anti-TWEAK-PE (120005), anti-CD11b-PerCP/cy5.5 (45-0112-80), anti-Ly6G-PE-CY7 (25-9668-82), anti-CD11b-PE-CY7 (25-0118-42), anti-CD3-APC (17-0032-82), anti-Ly6C-APC (17-5932-82), and L/D-APC-CY7 (L34974). TWEAK-PE was purchased from BioLegend (California, USA), while other antibodies were purchased from eBioscience (California, USA). Surface staining was used for the listed antibodies except CD68-AF488, where an intracellular staining was applied. For intracellular staining, the samples were fixed and permeabilized using fixation buffer (88–8824, eBioscience, California,

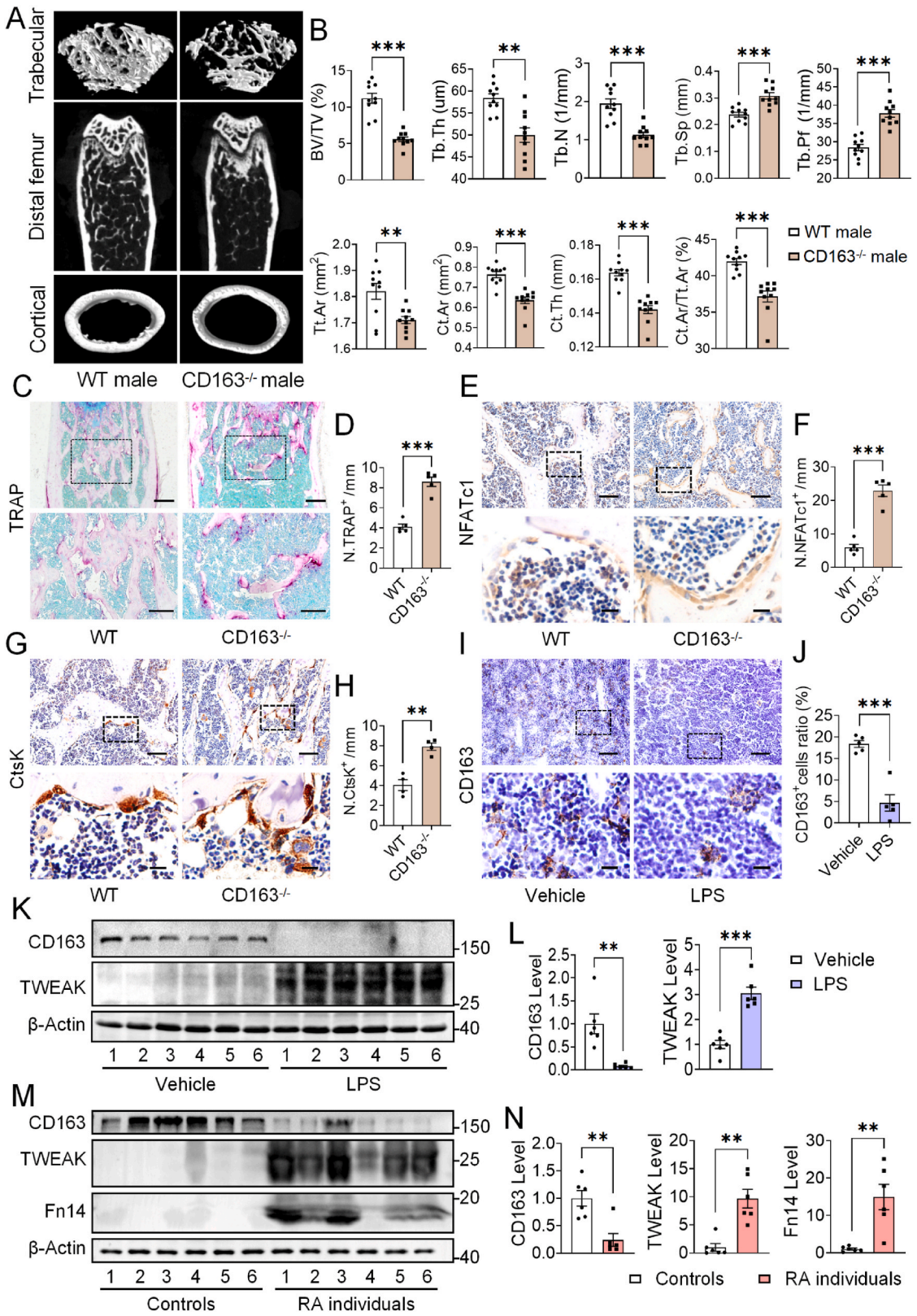

Fig. 1. CD163 regulates bone homeostasis and its level is reduced in inflammatory bone loss. (A, B) Representative μCT images and quantification of the distal trabecular bone and middle cortical bone of femora from CD163$^{-/-}$ male mice or their WT male littermates. (C, D). Representative images and quantification of TRAP staining from CD163$^{-/-}$ male mice or their WT male littermates. Scale bar: 200 μm (top), 100 μm (bottom). (E–H) Representative images and quantification of NFATc1 and CtsK from CD163$^{-/-}$ male mice or their WT male littermates. Scale bar: 50 μm (top), 10 μm (bottom). (I, J) Representative images and quantification of CD163 from mice treated with or without LPS. Scale bar: 50 μm (top), 10 μm (bottom). (K, L) Representative immunoblotting and quantification of CD163 and TWEAK in the bone marrow contents from mice treated with or without LPS. (M, N) Representative immunoblotting and quantification of CD163, TWEAK, and Fn14 in the bone marrow contents from RA individuals or controls. Dots represent individual mice or human samples. The data are presented as mean ± s. e.m., $*p < 0.05$, $**p < 0.01$, $***p < 0.001$.

USA). Stained cells were detected using Navios Flow Cytometer (Beckman Coulter, Miami, USA) and data were analyzed using FlowJo software version 10 (FlowJo LLC, OR, USA).

2.9. Cell culture, treatments, and OC differentiation

As previously described [36], bone marrow cells (BMCs) were isolated from the femora and tibias of male mice aged 4–6 weeks and cultured in α-MEM (AMM1001, Amizona Scientific LLC, Hangzhou, China) supplemented with 10 % FBS (10099141, Gibco, California, USA) and 1 % penicillin-streptomycin (15140122, Gibco, California, USA) for 24 h. Non-adherent cells were collected and further cultured with M-CSF (30 ng/mL, 51112-MNAH, SinoBiological, Beijing, China) for 48 h to induce OCPs. In some experiments, OCPs or BMCs were stimulated with rTWEAK (50174-M15H), rCD163 (RP02115), ATA (50 μM, HY-122575), or Dex (0.1 μM, HY-14648A) *in vitro*. For OC differentiation, OCPs were cultured with M-CSF (30 ng/mL) and RANKL (100 ng/mL, AM10004-050, Amizona Scientific LLC, Hangzhou, China). The medium was refreshed every 3 days. After 4–6 days, the cells were fixed and stained using the Tartrate Resistant Acid Phosphatase (TRAP) Kit (AMK1002-005, Amizona Scientific LLC, Hangzhou, China) for TRAP, or immuno-stained with AbFluor™ 594-Phalloidin (BMD0084, Abbkine, Wuhan, China) to detect actin belt. $TRAP^+$ OCs with three or more nuclei were counted.

For bone resorption assay, non-adherent cells were seeded on bone slices (AMB1001, Amizona Scientific LLC, Hangzhou, China) in the 24-well plates at a density of 1×10^5 cells per well and cultured in a growth medium containing 10 % FBS and M-CSF (50 ng/mL) for 24 h. OCPs were stimulated to differentiate into OCs with M-CSF (50 ng/mL) and RANKL (100 ng/mL) for 10 days. Bone slices were washed with 6 % sodium hypochlorite and deionized water. The absorption pit area on the dried bone slices was examined through a scanning electron microscope and quantified utilizing ImageJ software (ImageJ 1.53).

2.10. Quantitative real-time PCR

Total RNA was extracted from the bone marrow of the mice using RNAiso PLUS (9109, Takara, Shiga, Japan). Reverse transcription into cDNA was performed using PrimeScript™ RT reagent kit (RR037A, Takara, Shiga, Japan). Quantitative real-time PCR was performed using TB Green® *Premix Ex Taq*™ II (RR82LR, Takara, Shiga, Japan) on QuantStudio5 (Applied Biosystems, USA). *Actb* genes were utilized as an internal control, and the fold-change values were calculated by normalizing to control samples. The relative amount of each gene was calculated using the $2^{-\Delta\Delta CT}$ method. The following PCR primers for mouse samples were used:

Rankl Forward: 5′-ACCAGCATCAAAATCCCAAG-3′; *Rankl* Reverse: 5′-TTTGAAAGCCCCAAAGTACG-3′; *Opg* Forward: 5′-GAGAGTGAGGCAGGCTAT-3′; *Opg* Reverse: 5′-TGTGAGGAGAGGAAGGAAG-3′; *Actb* Forward: 5′-GCTTCTTTGCAGCTCCTTCGTT-3′; *Actb* Reverse: 5′-CGGAGCCGTTGTCGACGACC-3′.

2.11. Western blotting

Bone marrow tissues or cells were extracted using RIPA lysis buffer (89901, Thermo Fisher Scientific, Massachusetts, USA) supplemented with protease inhibitor (HY-K0010, MedChemExpress, New Jersey, USA), phosphatase inhibitor (HY-K0023, MedChemExpress, New Jersey, USA), and 1 mM phenylmethylsulfonyl fluoride (PMSF-RO, Sigma–Aldrich, Missouri, USA). Protein concentrations were measured using the Pierce Bicinchoninic Acid protein assay kit (23225, Thermo Fisher Scientific, Massachusetts, USA) and then equal amounts of protein extract were loaded on 10 % or 12.5 % SDS-PAGE gels, transferred onto 0.45 μm or 0.2 μm PVDF membranes (IPVH00010, ISEQ00010, Merck Millipore, New Jersey, USA), and blocked with 5 % bovine serum albumin (A9647, Sigma–Aldrich, Missouri, USA). The membranes were incubated with primary antibodies at 4 °C overnight with gentle agitation. The membranes were then washed three times in TBST for 10 min each prior to incubating with HRP-conjugated secondary antibodies for 1 h at room temperature. Immunoblots were detected using the Pierce™ ECL Plus Western Blotting Substrate (32134, Thermo Fisher Scientific, Massachusetts, USA) and visualized with a chemiluminescence instrument (Guangzhou Ewell Bio-Technology, Guangzhou, China). The primary antibodies included anti-NFATc1 (A1539), anti-CtsK (A1782), anti-CD163 (16646-1-AP), anti-TWEAK (DF7444), anti-Fn14 (ET1611-93), anti-p-ERK1/2 (ET1603-22, HuaBio, Hangzhou, China), anti-ERK1/2 (ET1601-29, HuaBio, Hangzhou, China), anti-p-JNK (ET1609-42, HuaBio, Hangzhou, China), anti-JNK (ET1601-28, HuaBio, Hangzhou, China), anti-p-P38 (ER2001-52, HuaBio, Hangzhou, China), anti-P38 (ET1602-26, HuaBio, Hangzhou, China), anti-p-IκBα (ET1609-78, HuaBio, Hangzhou, China), anti-IκBα (4812, CST, Massachusetts, USA), anti-p-P65 (3033, CST, Massachusetts, USA), anti-P65 (T55034, Abmart, Shanghai, China), anti-β-Actin (T40104, Abmart, Shanghai, China), and anti-β-Tubulin (FD0064, Fude Biological Technolog, Hangzhou, China). The secondary antibodies included HRP Conjugated Goat anti-Mouse IgG Goat Polyclonal Antibody (HA1006, Huabio, Hangzhou, China) and HRP Conjugated Goat anti-Rabbit IgG Goat Polyclonal Antibody (HA1001, Huabio, Hangzhou, China).

2.12. RNA interference

For Fn14 transfection, three siRNA candidates against Fn14 were produced by RIBBIO (Guangzhou, China). As previously described [37], non-adherent cells were seeded in 24-well plates at a density of 1×10^5 cells per well and cultured in a growth medium supplemented with 15 % FBS and M-CSF (30 ng/mL) until 70 % confluence was achieved. OCPs were then transfected with either Fn14 inhibitors or inhibitor controls for 24 h using the Lipofectamine 3000 reagent (L3000008, Thermo Fisher Scientific, Massachusetts, USA). After a 24-h interval, the osteoclast-inducing medium, which contained M-CSF (30 ng/mL) and RANKL (100 ng/mL), was replaced to initiate OC formation. The transfection efficiency was validated using Western blotting.

2.13. Statistical analysis

GraphPad Prism Software (v8.3.0, CA, USA) was used to perform statistical analysis. Comparisons between two groups were performed using unpaired two-tailed Student's t-tests. The Mann–Whitney U test was used for nonparametric analysis. Comparisons between three or more groups were performed using one-way analysis of variance (ANOVA) with Tukey's test. All data are expressed as mean ± s. e.m., p values < 0.05 were considered statistically significant ($^*p < 0.05$, $^{**}p < 0.01$, $^{***}p < 0.001$).

3. Results

3.1. CD163 regulates bone homeostasis and its level is reduced in inflammatory bone loss

To investigate the role of CD163 in bone homeostasis, we collected femora from $CD163^{-/-}$ mice and their WT littermates for μCT analysis. Mice deficient in CD163, either male or female, exhibited a severe

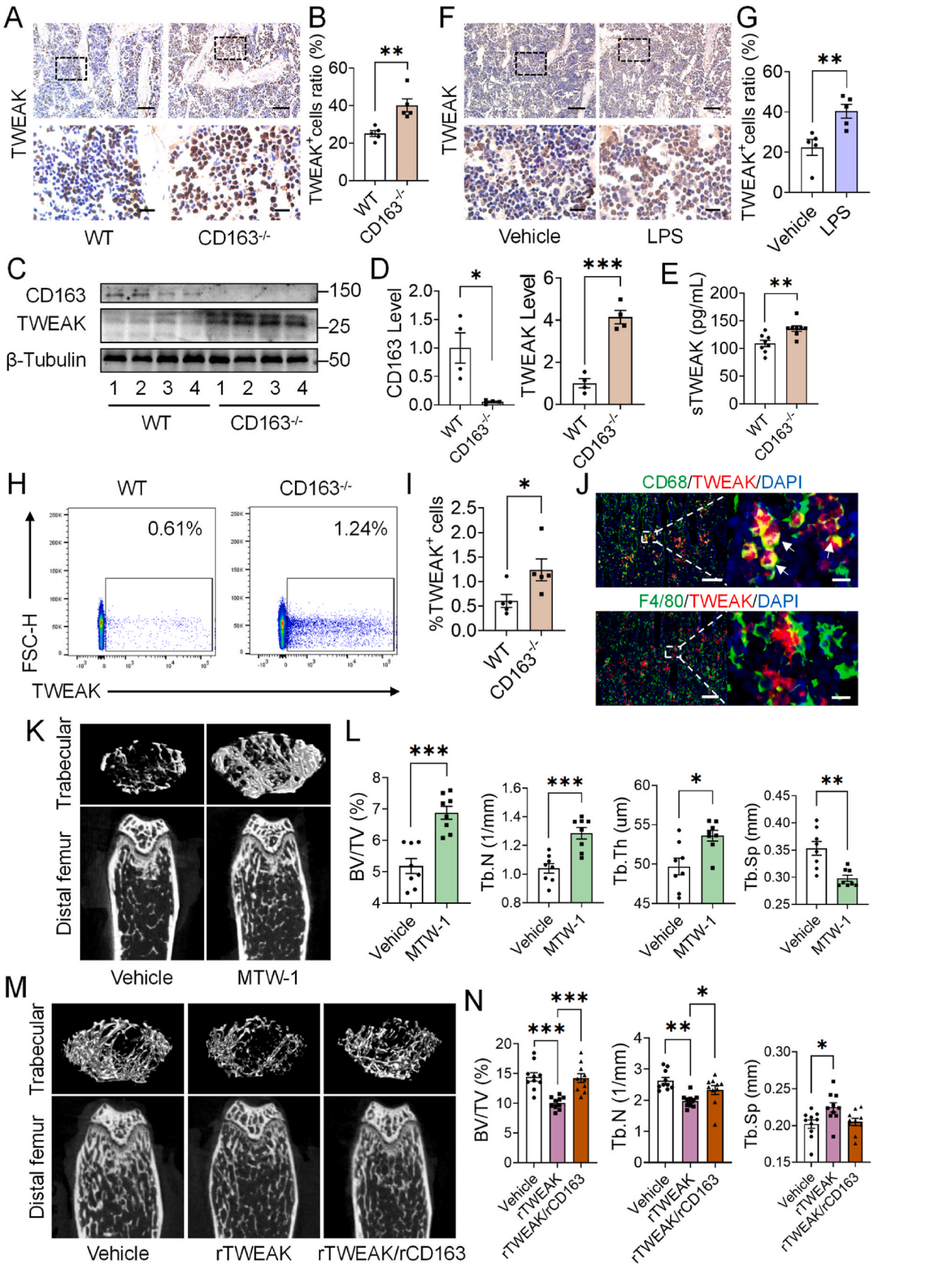

(caption on next page)

Fig. 2. TWEAK mediates the phenotype of osteoporosis in CD163$^{-/-}$ mice. (A, B) Representative images and quantification of TWEAK from CD163$^{-/-}$ male mice or their WT male littermates. Scale bar: 50 μm (top), 10 μm (bottom). (C, D) Representative immunoblotting and quantification of CD163 and TWEAK from CD163$^{-/-}$ male mice or their WT male littermates. (E) Quantification of sTWEAK level in the peripheral circulation using ELISA. (F, G) Representative images and quantification of TWEAK from mice treated with or without LPS. Scale bar: 50 μm (top), 10 μm (bottom). (H, I) Representative images and quantification for proportion of TWEAK^{+} cells in BMCs from CD163$^{-/-}$ male mice or their WT male littermates. The numbers in the upper right corner represent the average proportion of TWEAK^{+} cells. (J) Representative images of TWEAK^{+} (red), CD68^{+} (green), and F4/80^{+} (green) cells from CD163$^{-/-}$ mice. White arrow heads: the CD68-and TWEAK- double positive cells. Nuclei were stained with DAPI (blue). Scale: 50 μm (left), 10 μm (right). (K, L) Representative μCT images and quantification of femora from CD163$^{-/-}$ mice treated with or without MTW-1. (M, N) Representative μCT images and quantification of femora from WT mice treated with 0.1%BSA (Vehicle), rTWEAK, or rTWEAK plus rCD163. Dots represent individual mice. The data are presented as mean ± s. e.m., $*p < 0.05$, $**p < 0.01$, $***p < 0.001$. (For interpretation of the references to colour in this figure legend, the reader is referred to the Web version of this article.)

osteoporotic phenotype with a marked reduction in both trabecular and cortical bone mass (Fig. 1A and B, Fig. S1A and B). CD163 deficiency caused reductions in trabecular bone volume (BV/TV), trabecular thickness (Tb.Th), trabecular number (Tb.N), total cortical bone area (Tt.Ar), cortical bone area (Ct.Ar), cortical thickness (Ct.Th), and cortical bone cross-sectional area fraction (Ct.Ar/Tt.Ar) (Fig. 1A and B). In contrast, trabecular separation (Tb.Sp) and trabecular bone pattern factor (Tb.Pf) increased in CD163$^{-/-}$ mice (Fig. 1B). Further analysis was performed to determine whether bone loss following CD163 knockdown was linked to bone formation or bone resorption. As shown in Fig. 1C, there was a noteworthy increase in the number of TRAP-positive OCs per trabecular bone surface in CD163$^{-/-}$ mice compared to WT littermates (Fig. 1C and D). Furthermore, CD163 deficiency led to a significant elevation in the expression of NFATc1 and CtsK, which are associated with OC differentiation and function (Fig. 1E–H). Conversely, there was no significant alteration in the number of Ocn-positive cells per trabecular bone surface between the two groups (Fig. S2A and B). These results indicate that excessive osteoclastogenesis is the main cause of decreased bone mass observed in CD163$^{-/-}$ mice.

Given the increased abundance of OCs following CD163 knockdown, we assessed the osteoclastogenic capacity of OCPs from CD163$^{-/-}$ mice or their WT littermates *in vitro*. However, the numbers of multinucleated TRAP^{+} cells and actin belt formation were significantly reduced in OCPs from CD163$^{-/-}$ mice (Fig. S2C and D). The protein levels of NFATc1 and CtsK were also decreased in CD163 knockout OCs (Fig. S2E and F). This appears to counter the phenotype of bone loss and OC over-activation observed in CD163$^{-/-}$ mice *in vivo*. Furthermore, the CD163 protein level gradually declined and became completely undetectable by day 3 during the induction of OCPs formation by WT-derived BMCs (Fig. S2G and H), which is consistent with previous studies [19]. The expression of CD163 was also not detected in subsequent experiments where RNAKL was added to induce OC differentiation (Fig. S2I). Besides, rCD163 did not promote RANKL-dependent OC differentiation *in vitro* (Fig. S2J and K). These data suggest that the underlying cause of osteoporosis and OC over-activation in CD163$^{-/-}$ mice is not a direct effect of CD163 on OC differentiation. Instead, it is postulated that other factors contribute to OC over-activation following CD163 knockdown.

We then investigated the in situ expression of CD163 in bone tissues of pathological bone loss. LPS is typically employed to construct models of systemic inflammatory osteoporosis [38], and we successfully established an LPS-induced chronic inflammatory bone loss model with excessive osteoclastogenesis, as indicated by the decreased BV/TV and Tb.N, as well as the increased Tb. Sp, Tb. Pf, and the number of TRAP-positive OCs (Fig. S2L-O). Intriguingly, the in situ expression of CD163 in bone tissue was significantly lower in the LPS-treated group compared with vehicle group, whereas its expression in the estrogen-deficient osteoporosis or age-related osteoporosis groups did not differ from those in the control group (Fig. 1I and J, Fig. S3A-D). Immunoblotting analysis of bone marrow lysates also confirmed a significant reduction in CD163 expression in LPS-treated mice and RA individuals (Fig. 1K–N). In conclusion, these findings suggest that CD163 plays an essential role in maintaining bone homeostasis by indirectly regulating osteoclastogenesis, independently of gender or age. And its expression is compromised during inflammatory bone loss.

3.2. TWEAK mediates the phenotype of osteoporosis in CD163$^{-/-}$ mice

To investigate the mechanisms underlying bone loss in CD163$^{-/-}$ mice, we analyzed the expression of TWEAK, a ligand of CD163, which is predominantly expressed on leukocytes. We observed that the in situ expression of TWEAK was significantly increased in CD163$^{-/-}$ mice (Fig. 2A and B). This was further confirmed by immunoblotting analysis of bone marrow lysates (Fig. 2C and D). Consistent with these findings, the concentration of sTWEAK in the peripheral circulation of CD163$^{-/-}$ mice was significantly higher compared to WT littermates (Fig. 2E). TWEAK was also significantly up-regulated in the LPS-induced chronic inflammatory bone loss (Fig. 1K and L, Fig. 2F and G). Furthermore, we found that the expression of TWEAK was significantly higher in bone marrow samples obtained from sites adjacent to inflamed joints in individuals with RA (Fig. 1M and N). Besides, Fn14, another receptor whose affinity for TWEAK is higher than CD163 [39], was significantly elevated by approximately 14-fold (Fig. 1M and N). To further clarify the cell types that express TWEAK, we used flow cytometry to identify the level of TWEAK expression on B cells, T cells, monocytes, macrophages, and neutrophils. Mouse bone marrow macrophages are a population of highly heterogeneous and plastic macrophage lineage cells, exhibiting the capacity to alter their phenotype in response to environmental signals [40–42]. Therefore, two commonly employed markers for the identification of mouse macrophages, namely CD68 and F4/80 [43,44], were evaluated concurrently. As shown in Fig. 2H, we reconfirmed that the proportion of TWEAK^{+} cells in total BMCs of CD163$^{-/-}$ mice was notably higher compared to those of WT littermates (Fig. 2H and I). Furthermore, CD68^{+} TWEAK^{+} cells accounted for approximately 75 % of TWEAK^{+} cells, which was higher than that of other immune cell types, suggesting that TWEAK is mainly expressed on the CD68^{+} macrophages (Fig. S4A and B). Since TWEAK was predominantly expressed on CD68^{+} macrophages, fluorescence co-staining analysis was performed to validate these findings. As expected, TWEAK^{+} cells were primarily combined with CD68^{+} macrophages (Fig. 2J), which is consistent with previous literature reports [45,46].

To assess whether TWEAK mediates the osteoporotic phenotype of CD163$^{-/-}$ mice, we treated the mice with either a TWEAK-blocking antibody (MTW-1) or isotype IgG. MTW-1 effectively prevented bone loss in CD163$^{-/-}$ mice after 4 weeks of treatment, as assessed by elevated BV/TV, Tb.N, and Tb.Th, as well as decreased Tb. Sp (Fig. 2K and L). Furthermore, after administering intraperitoneal rTWEAK to WT

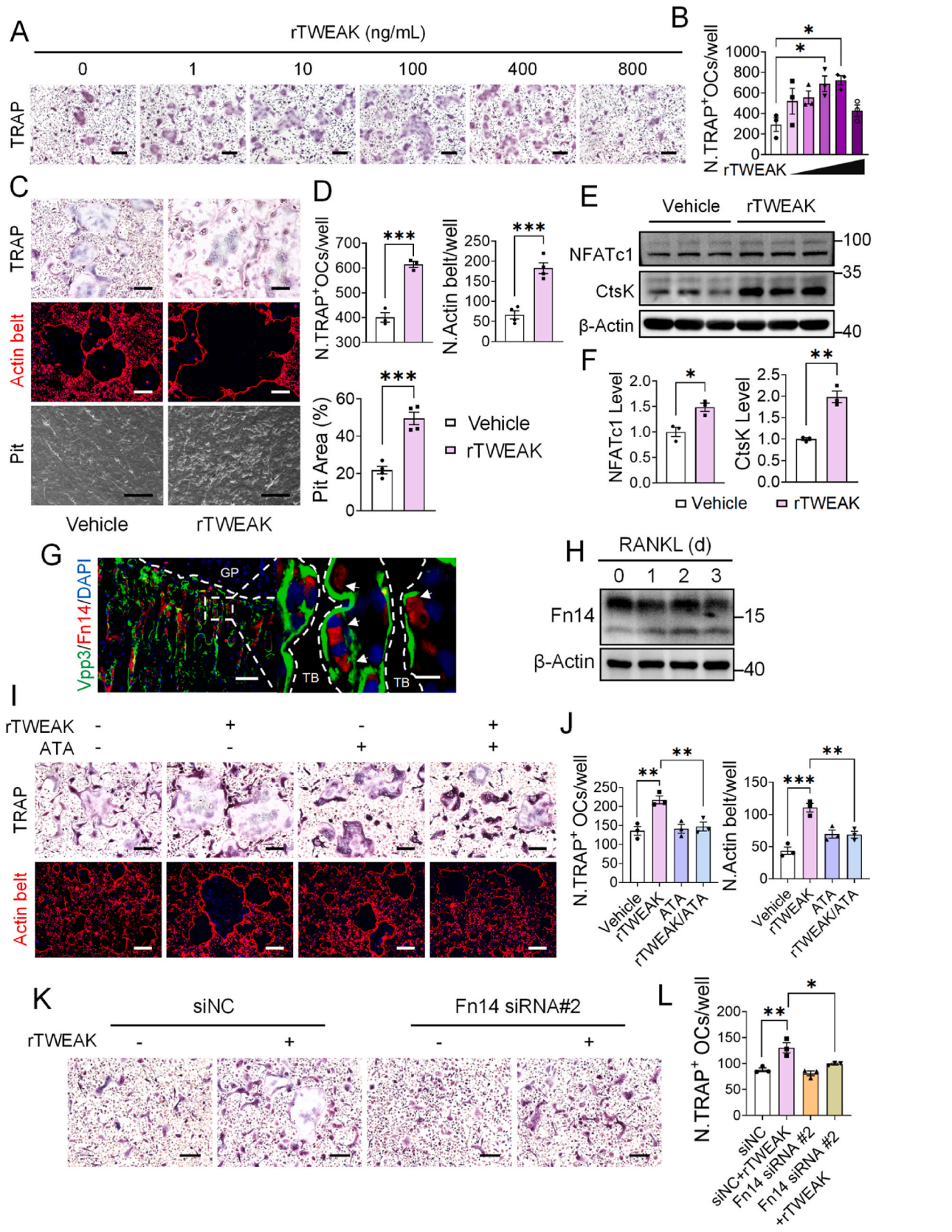

(caption on next page)

Fig. 3. TWEAK partners with RANKL to enhance osteoclastogenesis via the Fn14 receptor. (A, B) Representative images and quantification of TRAP staining in OCPs from WT mice treated with or without rTWEAK (1–800 ng/mL). Scale bar: 200 μm. (C, D) Representative images and quantification of TRAP staining (top), actin belt (middle), and resorption pit (bottom) in OCPs from WT mice treated with or without rTWEAK (100 ng/mL). Scale bar: 200 μm. (E, F) Representative immunoblotting and quantification of NFATc1 and CtsK in OCPs from WT mice treated with or without rTWEAK (100 ng/mL) for 3 days. (G) Representative images showing metaphyseal OCs (Vpp3, green) and $Fn14^+$ (red) cells from WT mice. White arrow heads: the Fn14-and Vpp3-double positive cells. Nuclei were stained with DAPI (blue). Scale: 50 μm (left) and 10 μm (right). (H) Protein level of Fn14 during the induction of OC formation *in vitro*, collected from WT mice. (I, J) Representative images and quantification of TRAP staining (top) and actin belt (bottom) in OCPs from WT mice treated with 0.1%BSA (Vehicle), rTWEAK (100 ng/mL), ATA (50 μM), or rTWEAK (100 ng/mL) plus ATA (50 μM). Scale bar: 200 μm. (K, L) Representative images and quantification of TRAP staining in Fn14 transfected OCPs from WT mice treated with or without rTWEAK (100 ng/mL). Scale bar: 200 μm. GP, growth plate. TB, trabecular bone. Dots represent biological replicates. The data are presented as mean ± s. e.m., $*p < 0.05$, $**p < 0.01$, $***p < 0.001$. (For interpretation of the references to colour in this figure legend, the reader is referred to the Web version of this article.)

mice for 4 weeks, uCT analysis revealed a significant bone loss in rTWEAK-treated mice, with decreased BV/TV and Tb.N, as well as the increased Tb. Sp (Fig. 2M and N). Interestingly, rTWEAK-induced bone loss was ameliorated by rCD163, as indicated by an increase in BV/TV and Tb.N (Fig. 2M and N). Taken together, these findings suggest that endogenous TWEAK, mainly derived from $CD68^+$ macrophages, is responsible for the bone loss observed in $CD163^{-/-}$ mice.

3.3. The CD163/TWEAK/Fn14 axis regulates osteoclastogenesis

We in turn investigated whether up-regulated TWEAK contributes to OCs-mediated bone loss in mice. The transcript levels of *Opg* and *Rankl* were examined in mouse bone marrow tissue in response to reports that TWEAK promotes *Rankl* expression. Although there was a 2-fold increase in *Rankl* levels in $CD163^{-/-}$ mice compared to those in WT littermates, the *Rankl/Opg* ratio was only slightly increased with no statistical differences (Fig. S5A and B), suggesting that bone loss caused by CD163 deficiency is not associated with a disruption of the *Rankl/Opg* ratio. Next, we investigated the optimal concentration of rTWEAK for promoting RANKL-dependent osteoclastogenesis, as rTWEAK alone was unable to induce OC formation (Fig. S5C). rTWEAK promoted OC differentiation in a concentration-dependent manner at low concentrations, but it inhibited OC differentiation at high concentrations (Fig. 3A and B). Therefore, the concentration of 100 ng/mL of rTWEAK was chosen for further studies due to its most notable effect in promoting osteoclastogenesis. rTWEAK promoted OC differentiation of OCPs from both WT (Fig. 3C and D) and $CD163^{-/-}$ mice (Fig. S5D and E), as the number of multinucleated $TRAP^+$ cells and actin belt formation were significantly increased in the rTWEAK-treated groups. In parallel, the protein levels of NFATc1 and CtsK were also increased in the groups with rTWEAK (Fig. 3E and F, Fig. S5F and G). Furthermore, rTWEAK promoted bone resorption capability *in vitro* (Fig. 3C and D).

Fn14, a functional receptor for TWEAK, is widely expressed in various tissues and cell types. We next explored whether OCs express the TWEAK receptor, Fn14, and whether Fn14 was critical in mediating the pro-osteoclastic effect of TWEAK. As shown in Fig. 3G, Fn14 was recombined in the OCs in the metaphysis (Fig. 3G). Fn14 was also detected at different stages of OC differentiation *in vitro* (Fig. 3H, Fig. S5H). Furthermore, the pro-osteoclastic effect of TWEAK was inhibited by ATA, an inhibitor of TWEAK/Fn14 signaling (Fig. 3I and J) [47,48]. The effect of TWEAK in promoting OC formation via Fn14 was further confirmed by suppressing the expression of Fn14 on OCPs with Fn14 siRNA, resulted in a reduction of the number of multinucleated $TRAP^+$ cells (Fig. 3K and L, Fig. S5I). These data provide evidence that TWEAK, via Fn14 receptor, synergizes with RANKL to promote OC differentiation and bone resorption capacity.

We then investigated the role of CD163 as a scavenger receptor in regulating the pro-osteoclastic effect of TWEAK/Fn14 signaling. First, we examined the optimal concentration of rCD163 required to inhibit TWEAK/Fn14-mediated osteoclastogenesis, and found that TWEAK/Fn14-mediated osteoclastogenesis was significantly inhibited when the concentration ratio of rCD163: rTWEAK was 20: 1 (Fig. 4A and B). As shown in Fig. 4C, the number of multinucleated $TRAP^+$ cells and actin belt formation were significantly increased in the rTWEAK-treated group compared to the other groups. These effects were considerably suppressed in the group treated with a combination of rCD163 when the concentration ratio of rCD163: rTWEAK was 20:1 (Fig. 4C and D). Surprisingly, compared to the vehicle group, high concentrations of rCD163 (2000 ng/mL) alone also improved OC formation (Fig. 4C and D). Furthermore, the protein levels of NFATc1 and CtsK were decreased in the group treated with both rCD163 and rTWEAK compared to the group treated with rTWEAK alone (Fig. 4E and F).

It is well known that the binding of RANKL to RANK expressed on OCPs triggers intracellular signaling cascades, such as the MAPK and NF-κB signaling pathways, which are crucial for OC differentiation. Thus, we subsequently analyzed whether TWEAK-driven osteoclastogenesis occurred through the signaling cascades described above. As presented in Fig. 4G, the phosphorylation levels of MAPK family markers, including ERK1/2, JNK, and P38, were increased during the initial stages of OC differentiation induced by treatment with rTWEAK when compared to those of controls (Fig. 4G and H). Consistent with our previous findings, the phosphorylation levels of ERK1/2 and JNK were attenuated in the group treated with rTWEAK plus rCD163 compared with the group treated with rTWEAK alone (Fig. 4I and J). In contrast, TWEAK had less effect on RANKL-induced phosphorylation of IkBa and P65, suggesting that the NF-κB signaling pathway does not participate in the osteoclast-inducing properties of TWEAK (Fig. S6A and B). Overall, our findings suggest that the CD163/TWEAK/Fn14 axis regulates osteoclastogenesis through the MAPK signaling pathway.

3.4. Targeting the CD163/TWEAK/Fn14 axis protects mice against inflammatory bone loss

To investigate the clinical significance of the CD163/TWEAK/Fn14 axis in inflammatory bone loss and the potential efficacy of targeting this axis to prevent bone loss with translational implications, rCD163 was initially supplemented into $CD163^{-/-}$ mice. μCT analysis revealed that supplementation with rCD163 effectively rescued bone loss in both trabecular and cortical bones of $CD163^{-/-}$ mice, with increased BV/TV, Tb.Th, Tb.N, Tt. Ar, Ct. Ar, Ct. Th, and Ct. Ar/Tt.Ar, as well as decreased Tb. Sp and Tb. Pf (Fig. 5A and B). Given that Dex was capable of stabilizing CD163 expression (Fig. S2G and H) [19,49,50], coupled with the fact that Dex excess may lead to iatrogenic complications such as glucocorticoid-induced osteoporosis [51,52]. We proceeded to investigate whether LPS-induced chronic inflammatory bone loss could be ameliorated using the following interventions: rCD163, ATA, and Dex-L, respectively. Strikingly, rCD163, ATA, and Dex-L all significantly ameliorated LPS-induced chronic inflammatory bone loss after 4 weeks

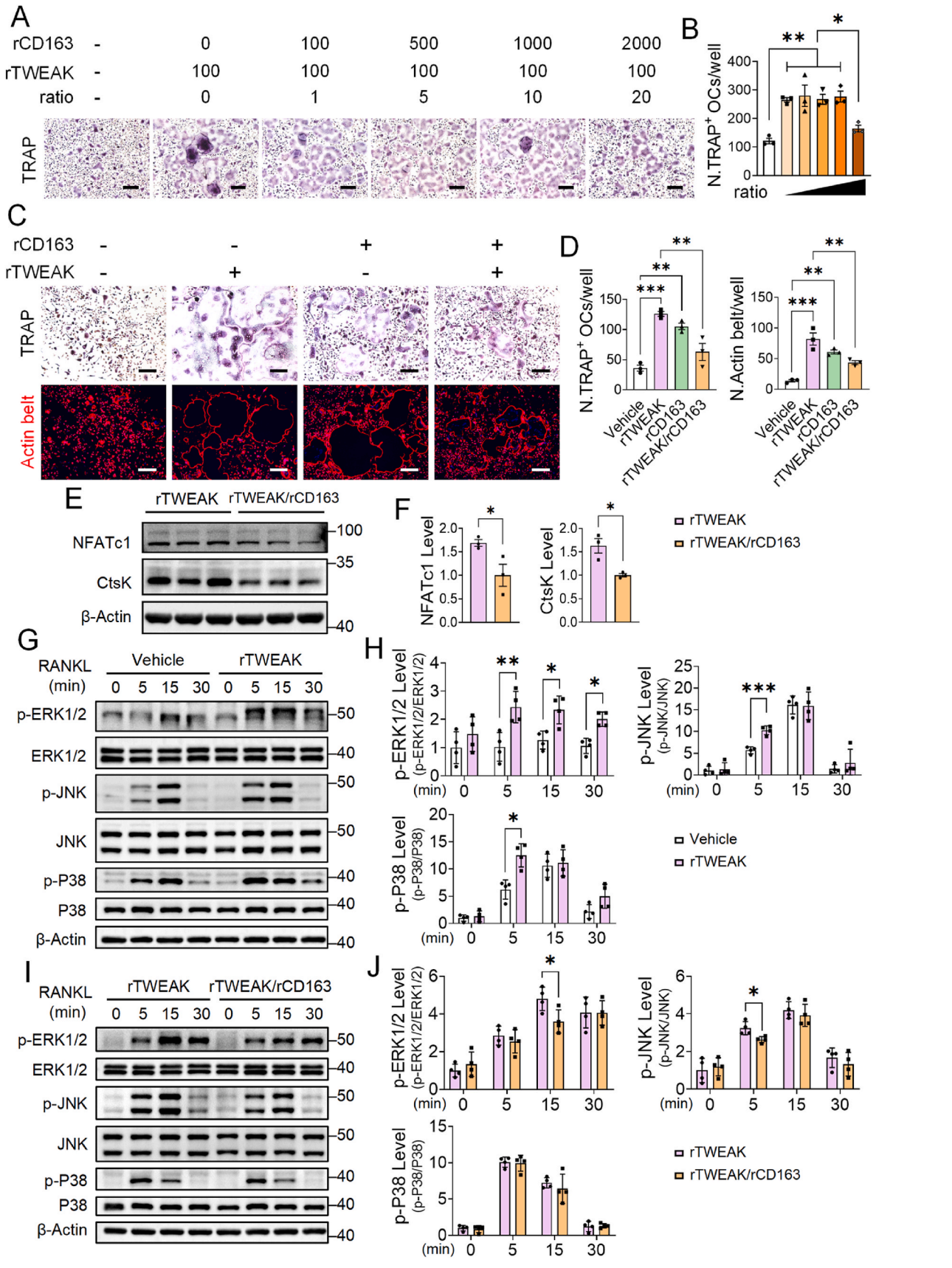

(caption on next page)

Fig. 4. The CD163/TWEAK/Fn14 axis regulates osteoclastogenesis through the MAPK signaling. (A, B) Representative images and quantification of TRAP staining in OCPs from WT mice treated with rTWEAK (100 ng/mL) or rTWEAK (100 ng/mL) plus rCD163 (100–2000 ng/mL). Scale bar: 200 μm. Ratio, the concentration ratio of rCD163: rTWEAK. (C, D) Representative images and quantification of TRAP staining (top) and actin belt (bottom) in OCPs from WT mice treated with 0.1 % BSA (Vehicle), rTWEAK (100 ng/mL), rCD163 (2000 ng/mL), or rTWEAK (100 ng/mL) plus rCD163 (2000 ng/mL). Scale bar: 200 μm. (E, F) Representative immunoblotting and quantification of NFATc1 and CtsK in OCPs from WT mice treated with rTWEAK (100 ng/mL) or rTWEAK (100 ng/mL) plus rCD163 (2000 ng/mL) for 3days. (G, H) Representative immunoblotting and quantification of three classical MAPKs (ERK1/2, JNK, and P38) in OCPs from WT mice treated with or without rTWEAK (100 ng/mL). (I, J) Representative immunoblotting and quantification of three classical MAPKs (ERK1/2, JNK, and P38) in OCPs from WT mice treated with rTWEAK (100 ng/mL) or rTWEAK (100 ng/mL) plus rCD163 (2000 ng/mL). Dots represent biological replicates. The data are presented as mean ± s. e.m., $*p < 0.05$, $**p < 0.01$, $***p < 0.001$.

of interventions, as evidenced by increased BV/TV and Tb.N, as well as decreased Tb. Sp and Tb. Pf (Fig. 5C and D). These results suggest that the CD163/TWEAK/Fn14 axis plays an important role in the pathogenesis of inflammatory bone loss and is a potential therapeutic target for the management of inflammatory bone loss.

4. Discussion

Inflammatory bone loss is a dominant cause of bone destruction and increased fracture risk in patients with chronic inflammatory diseases, including RA [1,4,8]. Although $CD163^+$ macrophages, a distinct subset of BMRMs, are expressed in numerous inflammatory and malignant diseases [53], little is known about their role in inflammatory bone loss. In this study, we demonstrate that $CD163^+$ BMRMs not only have anti-inflammatory roles, but also maintain bone homeostasis by indirectly regulating osteoclastogenesis through TWEAK. In patients with RA, $CD163^+$ macrophages are persistently expressed in inflamed synovial tissues [54,55]; moreover, CD163 deficiency has been reported to exacerbate the inflammatory response in collagen-induced arthritis and allergic contact dermatitis mouse models [29,30]. But our study showed a marked reduction in CD163 expression in the bone marrow of LPS-induced chronic inflammatory bone loss mice and RA patients. Combining our clinical samples and animal models initially showed that CD163 expression was lower in the trabecular bone region associated with RA than in cases of non-RA-associated bone loss, suggesting a potential relationship between reduced CD163 expression and inflammatory bone loss. Moreover, supplementation with exogenous rCD163 rescued both LPS-induced and CD163-deficiency-induced inflammatory bone loss.

CD163 functions as a multifunctional scavenger receptor involved in receptor-mediated endocytosis, such as Hp–Hb complexes and TWEAK [20,24,33]. TWEAK and Fn14 levels have been shown to be elevated in the synovium and serum of patients with RA and psoriatic arthritis [31,56]. A similar trend was also identified in our findings, including LPS-induced inflammatory bone loss and RA. Distinctly, we showed that endogenous TWEAK in the bone marrow was predominantly expressed by $CD68^+$ macrophages. High levels of ambient TWEAK exacerbate the pathologic response and tissue destruction in inflammatory and malignant diseases, such as psoriasis, autosomal dominant polycystic kidney disease, and hepatocellular carcinoma, and anti-TWEAK treatment effectively limits disease progression [45,57,58]. The underlying cause of osteoporosis and OC over-activation in $CD163^{-/-}$ mice was confirmed to be the promotion of OC differentiation via TWEAK following CD163 knockdown. Moreover, blocking TWEAK/Fn14 signaling contributed to rescue inflammatory bone loss. Additionally, the infusion of exogenous rTWEAK alone reproduced the osteoporotic phenotype in WT mice, whereas rCD163 rescued this phenotype. The results from our and previous studies indicate that TWEAK plays a crucial role in inflammatory bone loss, while CD163 degrades excessive TWEAK and prevents its detrimental effects on skeletal metabolism. It also reflects the body's self-regulatory mechanisms in response to inflammation.

Cytokines are key mediators of inflammatory bone loss, and their interdependence further contributes to robust osteoclastogenesis [9,13]. The impact of CD163/TWEAK on OC differentiation is controversial. Polek et al. report that TWEAK directly induces RAW264.7 differentiation into OCs independent of Fn14 and RANKL [59]. However, Dharmapatni et al. reported that TWEAK inhibits RANKL-induced hPBMC osteoclastogenesis [60]. In this study, we proved that TWEAK alone did not directly induce OC differentiation. However, TWEAK, via the receptor Fn14, enhanced RANKL-dependent osteoclastogenesis of bone marrow-derived OCPs in a concentration-dependent manner at low concentrations. Conversely, TWEAK had the opposite effect at high concentrations. TWEAK/Fn14 signaling triggers intracellular signaling cascades, such as NF-κB, MAPK, and Notch pathways [23,24]. Our data showed that TWEAK/Fn14 signaling synergistically promoted RANKL-dependent OC differentiation and bone resorption capability through the activation of downstream MAPK signaling, whereas CD163 scavenged TWEAK and reduced its impact on OCs (Fig. 6).

Although our findings indicate that targeting the CD163/TWEAK/Fn14 axis can prevent inflammatory bone loss, our study still has several limitations. M-CSF and RANKL are major factors in inducing OC differentiation; hence, once RANKL commits OCPs to the OC lineage, they will differentiate into OCs. In contrast, uncommitted OCPs exposed to antigens, such as LPS, continue as phagocytes [61]. In our data, OCPs from $CD163^{-/-}$ mice presented lower osteoclastogenesis *in vitro*. We propose that uncommitted OCPs are exposed to high level of TWEAK *in vivo*, which leads to inhibition of RANKL-RANK signaling to a certain extent. rCD163 could neutralize the pro-osteoclastic effect of rTWEAK, but it was also found to synergistically promote RANKL-induced OC differentiation at high concentration (2000 ng/mL). Nevertheless, we propose that such a high concentration of CD163 (2000 ng/mL) is non-physiological and much higher than the plasma level in healthy subjects (268 ng/mL) [62]. Moreover, as our study's clinical sample size was relatively limited, we intend to continue collecting more samples and even conduct cohort studies to validate our conclusions in the future.

In conclusion, our study reveals the contribution of the CD163/TWEAK/Fn14 axis in the pathogenesis of inflammatory bone loss. Therefore, besides direct cytokine arrest, supplementation with rCD163 or up-regulation of CD163 expression to enhance the body's anti-osteoporotic and anti-inflammatory capacity may be an alternative strategy for managing inflammatory bone loss.

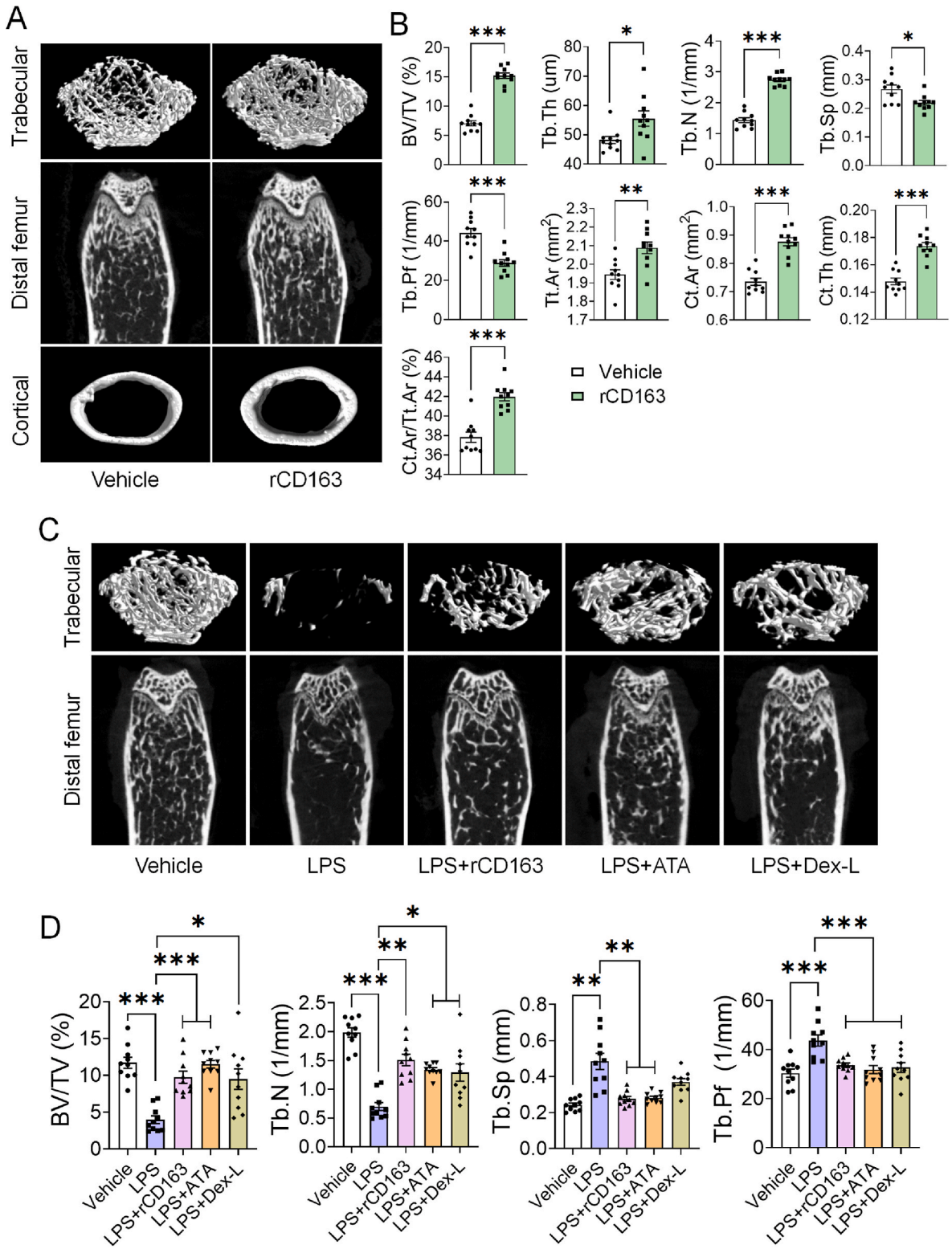

Fig. 5. Targeting the CD163/TWEAK/Fn14 axis protects mice against inflammatory bone loss. (A, B) Representative μCT images and quantification of the distal trabecular bone and middle cortical bone of femora from CD163$^{-/-}$ mice treated with or without rCD163. (C, D) Representative μCT images and quantification of the distal trabecular bone of femora in WT mice treated with PBS (Vehicle), LPS, LPS plus rCD163, LPS plus ATA, and LPS plus Dex-L, respectively. Dots represent individual mice. The data are presented as mean ± s. e.m., $^{*}p < 0.05$, $^{**}p < 0.01$, $^{***}p < 0.001$.

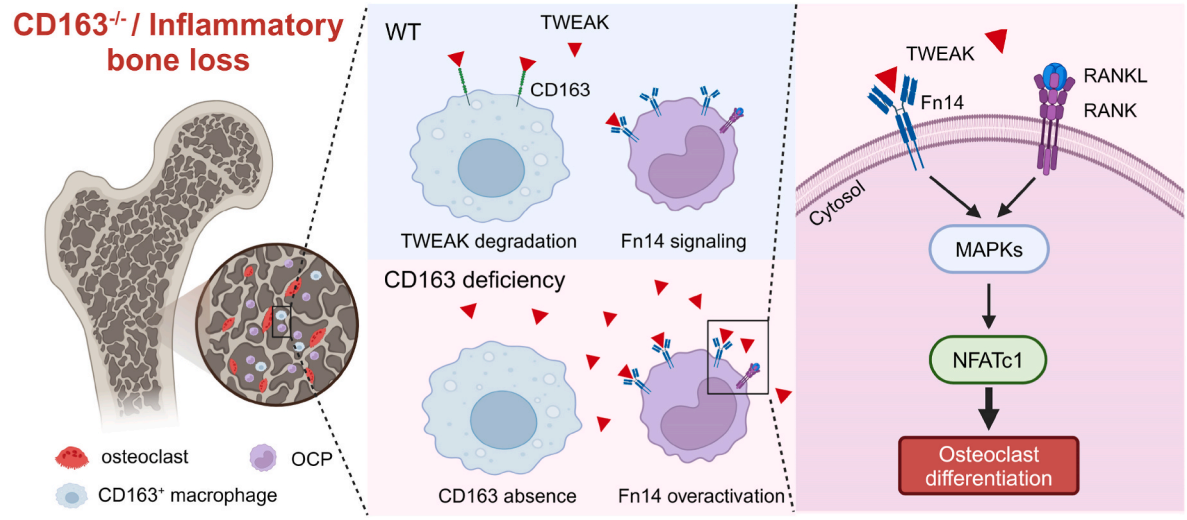

Fig. 6. The potential mechanism of CD163/TWEAK/Fn14 axis regulates osteoclastogenesis. Under normal conditions, $CD163^{+}$ bone marrow-resident macrophages compete with Fn14 to scavenge TWEAK, limiting the pro-osteoclastic effect of TWEAK/Fn14 signaling. However, in cases of inflammatory bone loss, the absence of CD163 in bone marrow-resident macrophages increases TWEAK availability, favoring its interaction with Fn14, synergistically promoting RANKL-dependent OC differentiation and bone resorption through the activation of downstream MAPK signaling.

Funding

This study was supported by grants from the Major Program of National Natural Science Foundation of China (81830079) and the National Natural Science Foundation of China (82272517, 31870954, and 82172197).

Ethics approval

Human bone marrow samples were obtained from patients with a diagnosis of rheumatoid arthritis after informed consent prior to surgery (Ethics Committee for Human Studies of Nanfang Hospital, Southern Medical University (NFEC-2020-074)). Patients were not involved in the design, or conduct, or reporting, or dissemination plans of this research. Animal experiments and procedures were approved by the Animal Care and Use Committee of Nanfang Hospital, Southern Medical University (NFYY-2022-0237).

Data availability

Data will be made available on request.

Declaration of competing interest

The authors declare that they have no known competing financial interests or personal relationships that could have appeared to influence the work reported in this paper.

Appendix A. Supplementary data

Supplementary data to this article can be found online at https://doi.org/10.1016/j.jot.2024.09.002.

References

[1] Redlich K, Smolen JS. Inflammatory bone loss: pathogenesis and therapeutic intervention. Nat Rev Drug Discov 2012;11:234–50.
[2] Goodman SB, Maruyama M. Inflammation, bone healing and osteonecrosis: from bedside to bench. J Inflamm Res 2020;13:913–23.
[3] Tsukasaki M, Takayanagi H. Osteoimmunology: evolving concepts in bone–immune interactions in health and disease. Nat Rev Immunol 2019;19:626–42.
[4] Komatsu N, Takayanagi H. Mechanisms of joint destruction in rheumatoid arthritis - immune cell-fibroblast-bone interactions. Nat Rev Rheumatol 2022;18:415–29.
[5] Foessl I, Dimai HP, Obermayer-Pietsch B. Long-term and sequential treatment for osteoporosis. Nat Rev Endocrinol 2023;19:520–33.
[6] Adami G. Regulation of bone mass in inflammatory diseases. Best Pract Res Clin Endocrinol Metabol 2022;36:101611.
[7] Ferbebouh M, Vallières F, Benderdour M, Fernandes J. The pathophysiology of immunoporosis: innovative therapeutic targets. Inflamm Res 2021;70:859–75.
[8] Mbalaviele G, Novack DV, Schett G, Teitelbaum SL. Inflammatory osteolysis: a conspiracy against bone. J Clin Invest 2017;127:2030–9.
[9] Herman S, Krönke G, Schett G. Molecular mechanisms of inflammatory bone damage: emerging targets for therapy. Trends Mol Med 2008;14:245–53.
[10] Tsukasaki M, Huynh NC-N, Okamoto K, Muro R, Terashima A, Kurikawa Y, et al. Stepwise cell fate decision pathways during osteoclastogenesis at single-cell resolution. Nat Metab 2020;2:1382–90.
[11] Tsukasaki M, Takayanagi H. Osteoclast biology in the single-cell era. Inflamm Regen 2022;42:27.
[12] Place DE, Malireddi RKS, Kim J, Vogel P, Yamamoto M, Kanneganti T-D. Osteoclast fusion and bone loss are restricted by interferon inducible guanylate binding proteins. Nat Commun 2021;12:496.
[13] Xia Y, Inoue K, Du Y, Baker SJ, Reddy EP, Greenblatt MB, et al. TGFβ reprograms TNF stimulation of macrophages towards a non-canonical pathway driving inflammatory osteoclastogenesis. Nat Commun 2022;13:3920.
[14] Cummings SR, San Martin J, McClung MR, Siris ES, Eastell R, Reid IR, et al. Denosumab for prevention of fractures in postmenopausal women with osteoporosis. N Engl J Med 2009;361:756–65.
[15] Boquete-Castro A, Gómez-Moreno G, Calvo-Guirado JL, Aguilar-Salvatierra A, Delgado-Ruiz RA. Denosumab and osteonecrosis of the jaw. A systematic analysis of events reported in clinical trials. Clin Oral Implants Res 2016;27:367–75.
[16] Popp AW, Zysset PK, Lippuner K. Rebound-associated vertebral fractures after discontinuation of denosumab-from clinic and biomechanics. Osteoporos Int 2016;27:1917–21.
[17] Law SK, Micklem KJ, Shaw JM, Zhang XP, Dong Y, Willis AC, et al. A new macrophage differentiation antigen which is a member of the scavenger receptor superfamily. Eur J Immunol 1993;23:2320–5.
[18] Pulford K, Micklem K, McCarthy S, Cordell J, Jones M, Mason DY. A monocyte/macrophage antigen recognized by the four antibodies GHI/61, Ber-MAC3, Ki-M8 and SM4. Immunology 1992;75:588–95.
[19] Fischer-Riepe L, Daber N, Schulte-Schrepping J, Véras De Carvalho BC, Russo A, Pohlen M, et al. CD163 expression defines specific, IRF8-dependent, immune-modulatory macrophages in the bone marrow. J Allergy Clin Immunol 2020;146:1137–51.
[20] Kristiansen M, Graversen JH, Jacobsen C, Sonne O, Hoffman HJ, Law SK, et al. Identification of the haemoglobin scavenger receptor. Nature 2001;409:198–201.
[21] Bover LC, Cardó-Vila M, Kuniyasu A, Sun J, Rangel R, Takeya M, et al. A previously unrecognized protein-protein interaction between TWEAK and CD163: potential biological implications. J Immunol 2007;178:8183–94.
[22] Maecker H, Varfolomeev E, Kischkel F, Lawrence D, LeBlanc H, Lee W, et al. TWEAK attenuates the transition from innate to adaptive immunity. Cell 2005;123:931–44.
[23] Winkles JA. The TWEAK-Fn14 cytokine-receptor axis: discovery, biology and therapeutic targeting. Nat Rev Drug Discov 2008;7:411–25.
[24] Ratajczak W, Atkinson SD, Kelly C. The TWEAK/Fn14/CD163 axis-implications for metabolic disease. Rev Endocr Metab Disord 2022;23:449–62.

[25] Gutiérrez-Muñoz C, Méndez-Barbero N, Svendsen P, Sastre C, Fernández-Laso V, Quesada P, et al. CD163 deficiency increases foam cell formation and plaque progression in atherosclerotic mice. Faseb J 2020;34:14960–76.
[26] Gupta RK, Gracias DT, Figueroa DS, Miki H, Miller J, Fung K, et al. TWEAK functions with TNF and IL-17 on keratinocytes and is a potential target for psoriasis therapy. Science immunology 2021;6:eabi8823.
[27] Mendez-Barbero N, Yuste-Montalvo A, Nuñez-Borque E, Jensen BM, Gutiérrez-Muñoz C, Tome-Amat J, et al. The TNF-like weak inducer of the apoptosis/fibroblast growth factor–inducible molecule 14 axis mediates histamine and platelet-activating factor–induced subcutaneous vascular leakage and anaphylactic shock. J Allergy Clin Immunol 2020;145. 583-96.e6.
[28] Moreno JA, Muñoz-García B, Martín-Ventura JL, Madrigal-Matute J, Orbe J, Páramo JA, et al. The CD163-expressing macrophages recognize and internalize TWEAK: potential consequences in atherosclerosis. Atherosclerosis 2009;207:103–10.
[29] Svendsen P, Etzerodt A, Deleuran BW, Moestrup SK. Mouse CD163 deficiency strongly enhances experimental collagen-induced arthritis. Sci Rep 2020;10:12447.
[30] Fujiwara Y, Ohnishi K, Horlad H, Saito Y, Shiraishi D, Takeya H, et al. CD163 deficiency facilitates lipopolysaccharide-induced inflammatory responses and endotoxin shock in mice. Clin Transl Immunology 2020;9:e1162.
[31] Park J-S, Kwok S-K, Lim M-A, Oh H-J, Kim E-K, Jhun J-Y, et al. TWEAK promotes osteoclastogenesis in rheumatoid arthritis. Am J Pathol 2013;183:857–67.
[32] Vincent C, Findlay DM, Welldon KJ, Wijenayaka AR, Zheng TS, Haynes DR, et al. Pro-inflammatory cytokines TNF-related weak inducer of apoptosis (TWEAK) and TNFalpha induce the mitogen-activated protein kinase (MAPK)-dependent expression of sclerostin in human osteoblasts. J Bone Miner Res 2009;24:1434–49.
[33] Akahori H, Karmali V, Polavarapu R, Lyle AN, Weiss D, Shin E, et al. CD163 interacts with TWEAK to regulate tissue regeneration after ischaemic injury. Nat Commun 2015;6:7792.
[34] Dou C, Ding N, Xing J, Zhao C, Kang F, Hou T, et al. Dihydroartemisinin attenuates lipopolysaccharide-induced osteoclastogenesis and bone loss via the mitochondria-dependent apoptosis pathway. Cell Death Dis 2016;7:e2162.
[35] Ma S-W, Huang X, Li Y-Y, Tang L-B, Sun X-F, Jiang X-T, et al. High serum IL-21 levels after 12 weeks of antiviral therapy predict HBeAg seroconversion in chronic hepatitis B. J Hepatol 2012;56:775–81.
[36] Yi SJ, Jang YJ, Lee S, Cho SJ, Kang K, Park JI, et al. TMBIM6 deficiency leads to bone loss by accelerating osteoclastogenesis. Redox Biol 2023;64:102804.
[37] Yang C, Tao H, Zhang H, Xia Y, Bai J, Ge G, et al. TET2 regulates osteoclastogenesis by modulating autophagy in OVX-induced bone loss. Autophagy 2022;18:2817–29.
[38] Bott KN, Feldman E, de Souza RJ, Comelli EM, Klentrou P, Peters SJ, et al. Lipopolysaccharide-induced bone loss in rodent models: a systematic review and meta-analysis. J Bone Miner Res 2023;38:198–213.
[39] Wang S, Li L, Cook C, Zhang Y, Xia Y, Liu Y. A potential fate decision landscape of the TWEAK/Fn14 axis on stem and progenitor cells: a systematic review. Stem Cell Res Ther 2022;13:270.
[40] Park MD, Silvin A, Ginhoux F, Merad M. Macrophages in health and disease. Cell 2022;185:4259–79.
[41] Beattie L, Sawtell A, Mann J, Frame TCM, Teal B, de Labastida Rivera F, et al. Bone marrow-derived and resident liver macrophages display unique transcriptomic signatures but similar biological functions. J Hepatol 2016;65:758–68.
[42] Gu Q, Yang H, Shi Q. Macrophages and bone inflammation. Journal of orthopaedic translation 2017;10:86–93.
[43] Deng R, Li C, Wang X, Chang L, Ni S, Zhang W, et al. Periosteal CD68(+) F4/80(+) macrophages are mechanosensitive for cortical bone formation by secretion and activation of TGF-β1. Adv Sci 2022;9:e2103343.
[44] Xu HT, Lee CW, Li MY, Wang YF, Yung PS, Lee OK. The shift in macrophages polarisation after tendon injury: a systematic review. Journal of orthopaedic translation 2020;21:24–34.
[45] Liu W, Gao L, Hou X, Feng S, Yan H, Pan H, et al. TWEAK signaling-induced ID1 expression drives malignant transformation of hepatic progenitor cells during hepatocarcinogenesis. Adv Sci 2023;10:e2300350.
[46] Dwyer BJ, Jarman EJ, Gogoi-Tiwari J, Ferreira-Gonzalez S, Boulter L, Guest RV, et al. TWEAK/Fn14 signalling promotes cholangiocarcinoma niche formation and progression. J Hepatol 2021;74:860–72.
[47] Burman P, Jaiswal R, Devi K, Moharana B. Aurintricarboxylic acid protects isoproterenol induced left ventricular hypertrophy by modulating TWEAK signaling. Cardiovasc Pathol 2022;61:107468.
[48] Roos A, Dhruv HD, Mathews IT, Inge LJ, Tuncali S, Hartman LK, et al. Identification of aurintricarboxylic acid as a selective inhibitor of the TWEAK-Fn14 signaling pathway in glioblastoma cells. Oncotarget 2017;8:12234–46.
[49] Koenen M, Culemann S, Vettorazzi S, Caratti G, Frappart L, Baum W, et al. Glucocorticoid receptor in stromal cells is essential for glucocorticoid-mediated suppression of inflammation in arthritis. Ann Rheum Dis 2018;77:1610–8.
[50] Keeler GD, Durdik JM, Stenken JA. Effects of delayed delivery of dexamethasone-21-phosphate via subcutaneous microdialysis implants on macrophage activation in rats. Acta Biomater 2015;23:27–37.
[51] Chotiyarnwong P, McCloskey EV. Pathogenesis of glucocorticoid-induced osteoporosis and options for treatment. Nat Rev Endocrinol 2020;16:437–47.
[52] Wang G, Ma C, Mo L, Chen J, Yuan J, Xu J, et al. Cycloastragenol prevents bone loss via inhibiting osteoclast activity in glucocorticoid-induced osteonecrosis of the femoral head: an in vivo study. Journal of orthopaedic translation 2024;45:178–87.
[53] Skytthe MK, Graversen JH, Moestrup SK. Targeting of CD163(+) macrophages in inflammatory and malignant diseases. Int J Mol Sci 2020;21.
[54] Baeten D, Møller HJ, Delanghe J, Veys EM, Moestrup SK, De Keyser F. Association of CD163+ macrophages and local production of soluble CD163 with decreased lymphocyte activation in spondylarthropathy synovitis. Arthritis Rheum 2004;50:1611–23.
[55] De Rycke L, Baeten D, Foell D, Kruithof E, Veys EM, Roth J, et al. Differential expression and response to anti-TNFalpha treatment of infiltrating versus resident tissue macrophage subsets in autoimmune arthritis. J Pathol 2005;206:17–27.
[56] van Kuijk AW, Wijbrandts CA, Vinkenoog M, Zheng TS, Reedquist KA, Tak PP. TWEAK and its receptor Fn14 in the synovium of patients with rheumatoid arthritis compared to psoriatic arthritis and its response to tumour necrosis factor blockade. Ann Rheum Dis 2010;69:301–4.
[57] Gupta RK, Gracias DT, Figueroa DS, Miki H, Miller J, Fung K, et al. TWEAK functions with TNF and IL-17 on keratinocytes and is a potential target for psoriasis therapy. Science immunology 2021;6:eabi8823.
[58] Cordido A, Nuñez-Gonzalez L, Martinez-Moreno JM, Lamas-Gonzalez O, Rodriguez-Osorio L, Perez-Gomez MV, et al. TWEAK signaling pathway blockade slows cyst growth and disease progression in autosomal dominant polycystic kidney disease. J Am Soc Nephrol 2021;32:1913–32.
[59] Polek TC, Talpaz M, Darnay BG, Spivak-Kroizman T. TWEAK mediates signal transduction and differentiation of RAW264.7 cells in the absence of fn14/TweakR: evidence for a second TWEAK receptor. J Biol Chem 2003;278:32317–23.
[60] Dharmapatni AA, Smith MD, Crotti TN, Holding CA, Vincent C, Weedon HM, et al. TWEAK and Fn14 expression in the pathogenesis of joint inflammation and bone erosion in rheumatoid arthritis. Arthritis Res Ther 2011;13:R51.
[61] Liu J, Wang S, Zhang P, Said-Al-Naief N, Michalek SM, Feng X. Molecular mechanism of the bifunctional role of lipopolysaccharide in osteoclastogenesis. J Biol Chem 2009;284:12512–23.
[62] Grannes H, Ueland T, Simeone P, Liani R, Guagnano MT, Aukrust P, et al. Liraglutide and not lifestyle intervention reduces soluble CD163 after comparable weight loss in obese participants with prediabetes or type 2 diabetes mellitus. Cardiovasc Diabetol 2024;23:146.